

# A Parametric Test Method for Analog Components in Integrated Mixed-Signal Circuits

M. Pronath, V. Gloeckel, H. Graeb

Institute of Electronic Design Automation, Technical University of Munich

## Abstract

In this paper, we present a novel approach to use test stimuli generated by digital components of a mixed-signal circuit for testing its analog components. A wavelet transform is applied to the response signal of the device under test (DUT). We will show, that in comparison to Fourier transform or no transform at all, particular properties of this transformation are advantageous for mixed-signal test and especially built-in self test.

We introduce a new method for test measurement selection based on a *non-deterministic parametric fault model* for analog circuits. This approach allows for noise and measurement error in testing. We show, how test quality can be optimized in the presented fault model. Our test methodology is demonstrated on an analog CMOS bandpass filter.

## 1 Introduction

The increasing trend towards integration of digital and analog components on the same chip has spawned growing attention to the test needs of mixed-signal ICs. After all, the price of an increasing number of devices is presently dominated by the cost of production testing. A major part of these testing costs are due to performance test of analog components.

Faults that occur in analog circuits are commonly classified into *catastrophic faults* (hard faults) caused e.g. by spot defects and *parametric faults* (soft faults) [1]. A circuit fails due to a parametric fault, if random fluctuations inherent to the manufacturing process lead to a significant performance loss that violates the circuit's specification. Mixed-signal test engineers and designers are primarily concerned with parametric faults because these faults are hard to distinguish from acceptable process variations [2, 3].

Most of the early work dealing with test design for analog circuits can be classified into two groups. The first group uses measurements of the specified performances only, and aims at minimizing test cost by optimal ordering of tests or by reducing the number of tests [3, 4]. The second group constructs a test set based on measurements that are regarded to be sensitive and reasonable, but do not necessarily include the specified performances of the circuit. Most of these approaches aim at the detection of catastrophic faults [5–7]. Recently, approaches aiming at the detection of parametric faults for LTI systems [9] and for arbitrary circuits [8] have been published.

Analog components that are embedded in a mixed-signal circuit impose harder restrictions on test methodologies than isolated analog components, since functional testing of analog circuits requires insertion of analog stimuli into the DUT as well as precise measurement of the circuit response. This often conflicts with the goal of dense integration. Support for testing by means of on-chip test structures may solve some of these problems. Research in this area showed results regarding on-chip support for generation of test stimuli as well as for evaluation of the DUT's output signals [9–12]. To circumvent the complexity of high-speed high-performance test equipment, some built-in self test (BIST) strate-

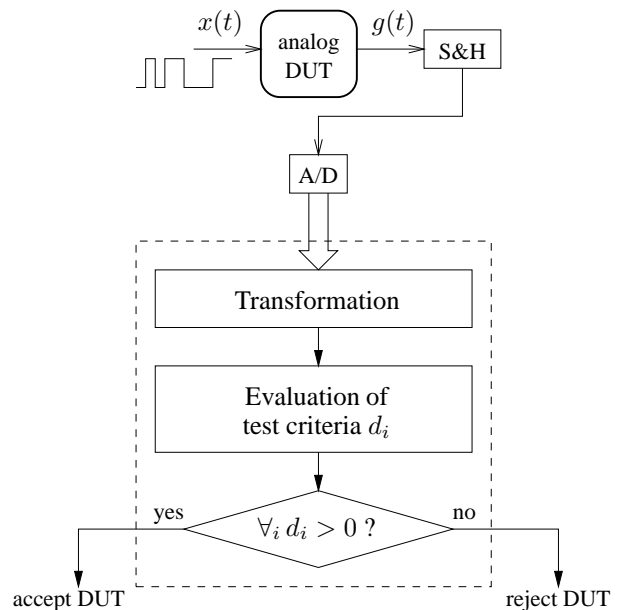


Figure 1: Test method

gies try to detect circuit faults by means of simple measurements performed by low-performance test circuitry that is integrated with the DUT [13, 14].

In this paper, we introduce a new method for test selection together with a parametric fault model that includes measurement errors and allows an optimization of test quality and test effectiveness (Section 3). We demonstrate our approach on a test method selected particularly with regard to BIST (Section 2). Important features of this method are simple generation of test stimuli, feasible on-chip evaluation of test measurements by wavelet transform, and a low sensitivity to measurement noise. Our test method is performed on an analog CMOS bandpass filter circuit. The circuit's specification regarding center frequency ( $f_0 > 17.5\text{MHz}$ ) and quality ( $Q > 15.5$ ) will be tested by means of a 10-bit, 1MSamples/s A/D-converter (ADC). The moderate performance of the ADC has been chosen to show that a test based on characteristic observations may yield an acceptable test quality in situations where the performance of a specified test equipment is insufficient for a full functional test, or where application of high-performance test structures is not feasible. In Section 5, we will show that wavelet transform may significantly increase test quality compared to Fourier transform or no transform.

## 2 Test method

Figure 1 shows our way to determine spectral coefficients that can be used for testing a DUT. A test stimulus  $x(t)$  as shown in Fig-

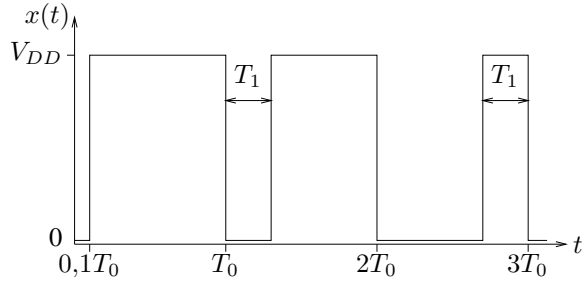


Figure 2: Test stimulus

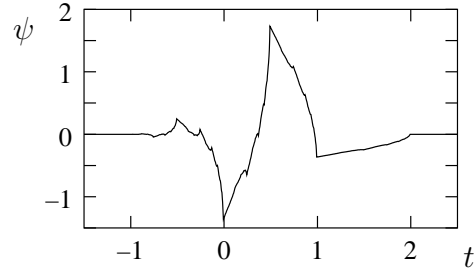


Figure 3: Daubechies wavelet

ure 2 is applied to the circuit. The test stimulus has been chosen particularly with regard to analog BIST in the digital environment of the DUT.  $x(t)$  can be generated by digital circuitry, and hence this test method needs no external signal generation or a complex integrated analog test signal generation. We assume the shape depicted in Fig. 2, that is defined by two parameters  $T_0, T_1$  and the rise/fall time  $t_r$ . In the example performed in Section 5,  $3T_0 \leq 60\mu s$ , which leads to a short overall testing time. Note that due to the large voltage swing of this digital input signal, the DUT cannot be treated as a linear time-invariant (LTI) system anymore.

The circuit's response  $g(t)$  is sampled and quantized, and then undergoes a wavelet transform. The resulting wavelet coefficients  $\circ$  are used to calculate a test result  $d_i$  for each specified performance  $f_i, i = 1 \dots n_f$ , that indicates whether the DUT satisfies this specification or not.

The test decision has to be made upon the output signal  $g(t)$  of the DUT, when the test stimulus  $x(t)$  is applied to it (Fig. 1). In  $g(t)$ , the information content may be condensed at discrete points (e.g. local extrema, poles and zeros, etc.) or spread over larger parts of the function (e.g. the global maximum or the mean value). In many applications that depend on the non-local information content, function transforms play an important role, since they may condense wide-spread information at a few discrete points. For example, with  $G(\omega)$  being the Fourier transform of  $g(t)$ , the integral  $\int_{-\infty}^{\infty} g(t) dt$  is  $G(0)$ .

A drawback of the Fourier transform is its handling of “semi-local” information content, i.e. a characteristic of limited extent in time like a slope or a spike. These properties are often of interest, and are detected more clearly by other transformations such as a windowed Fourier transformation or wavelet transformations. Wavelet transformations [15] as used in this work are based on a set of orthonormal basis functions  $\psi^{(a,b)}$  that are derived from a single function  $\psi$  by scaling and shifting

$$\psi^{(a,b)}(t) = |a|^{-1/2} \psi\left(\frac{t-b}{a}\right). \quad (1)$$

The wavelet transform  $\mathcal{W}_\psi\{g\} : \mathbb{R}^2 \rightarrow \mathbb{R}$  of a function  $g : \mathbb{R} \rightarrow \mathbb{R}$  is then

$$\mathcal{W}_\psi\{g\}(a,b) = c_\psi \int_{-\infty}^{\infty} g(t) \psi^{(a,b)}(t) dt, \quad (2)$$

with some constant value  $c_\psi$  that depends on the used basis function  $\psi$ . The basis function used in this work is the widely used Daubechies wavelet of second order (Fig. 3), since it yields an orthonormal basis for discrete transforms as well as a fast transform algorithm. In the case of sampled functions, a real-valued sequence  $\{g_n\}, 0 \leq n < N$ , is transformed into the mean value  $c_0$  and a set of coefficients  $d_k^m = \mathcal{W}_\psi\{g\}(2^m, k2^m)$  for  $1 \leq m \leq \log_2 N$  and  $0 \leq k < N/2^m$ , altogether  $N$  values.

In contrast to the Fourier transform, the basis functions of this transform have compact support. Thus, each of the resulting coefficients is influenced only by a part of  $g$  just like the coefficients of a windowed Fourier transform. Furthermore, algorithms for discrete transforms are available that make VLSI implementa-

tions feasible [12, 16]. For test measurements, wavelet coefficients have three important advantages over Fourier coefficients or time-domain measurements:

1. *SNR at high frequencies.* The high-frequency part of the spectrum of  $g(t)$  may either result from a long-time high-frequency oscillation (i.e. a global characteristic of  $g(t)$ ), or from steep slopes (i.e. an event-like characteristic of limited extent in time). A small transform window around an event like this contains all values of  $g(t)$  that contribute to the high-frequency coefficients, but only a small part of an inevitable noise floor that is induced by measurement errors. In this case, a wavelet transform yields a far better signal-to-noise ratio than the Fourier transform.

The test stimuli  $x(t)$  used in this approach induce high-frequency spectral components by steep slopes. Although this characteristic need not automatically be assumed to be valid for the output signal  $g(t)$ , this is probable for many kinds of circuits. Thus, by using the wavelet transform, higher frequency parts of the spectrum of  $g(t)$  can be utilized for making a test decision.

In contrast to a windowed Fourier transform that uses a window of constant width, the wavelet transform does not lead to a decrease of relative precision for higher frequencies and has a better time-domain resolution for fast events.

2. *Time-domain localization.* To keep the number of observations small, the employed transform must extract and concentrate important information of  $g(t)$  as good as possible. Unfortunately, the information content “when did event  $x$  happen” is distributed over the phase of all coefficients after Fourier analysis. Many test approaches that use the Fourier transform for test measurements hence consider only the magnitude of the result [17, 18]. Since this is not the case for the wavelet transform, time-domain localization of discrete events can be employed for making a test decision [19, 20].

3. *Fast transformation.* Fast discrete wavelet transform can be computed in  $O(n)$  operations, whereas fast Fourier transform can be computed in  $O(n \log_2 n)$  operations. In the example presented in Section 5, calculation of the Fourier coefficients took almost twice as long as calculation of the wavelet coefficients. Depending on the test equipment, calculation of the transform may dominate testing time.

### 3 Test design

#### 3.1 Selection of test measurements

In this section, we will present a new test selection procedure that combines the following features:

- parametric fault model based on specification
- selection of test groups
- measurement error considered
- ambiguity groups considered
- scalar minimization goal

Most of the previous work dealing with test selection for the detection of parametric faults consider an excessive statistical parameter variation a parametric fault. Hence, the authors concentrate on the relation between measurements and statistical parameters  $\mathbf{s}$ . The goal of selection algorithms is then a minimal subset of the measurements that allows a robust prediction of  $\mathbf{s}$  in a linear model [4, 21, 22].

In our approach, a parametric fault is defined as a violation of the circuit's specification. Since applying a single test stimulus to the circuit will yield a large number of characteristic observations, a test selection algorithm for  $\mathbf{o}$  has to consider that the observations cannot be selected independently from each other. Instead, they are divided into groups of observations (or *test points*  $tp_i$ ), each of which is to be measured separately. In our example, a test point denotes a certain test stimulus that is applied to the circuit. Each of the resulting spectral coefficients of the measured output signal is a characteristic observation.

The presented approach is based on a parametric fault model that builds up a relation between specifications  $f \geq f_b$  of the circuit (e.g.  $A_0 \geq 80\text{dB}$ ) and characteristic observations  $\mathbf{o}$ . Observations may be any measurable values of the circuit, and may include the specified performances. Observations  $\mathbf{o}$  and performances  $f$  vary between devices due to process fluctuations (e.g. oxide thickness or width/length fluctuation), which are modeled by using a vector of random variables  $\mathbf{s}$  for transistor model parameters (e.g.  $v_{th0}$ ,  $\text{tox}$ ,  $\text{lcorr}$ ). The measurement of  $\mathbf{o}$  is influenced by errors  $\boldsymbol{\varepsilon}$  induced by noise, sampling error or quantization error in the test equipment. In the following, the real value  $\mathbf{o}$  is considered different from its measured value  $\mathbf{o}'$ . The inclusion of measurement errors into the fault model leads to a *non-deterministic* description of the go/no-go test decision, because it allows for a DUT being classified differently in two subsequent measurements. The classification of a DUT during production test is indeterminate to a certain degree due to measurement errors and noise, which we take into account by a probability of acceptance that is less or equal to 1.

The test selection algorithm uses a model of  $\mathbf{o}$  and  $f$  that is linear in  $\mathbf{s}$ . Since the presented method aims at gaining information on  $f$  by measuring  $\mathbf{o}$ , the estimation error in that linear model is used as a quality measure of a selected set of measurements.

In the following,  $\mathbf{s} \sim N(\mathbf{0}, \mathbf{I})$  is assumed. Since the commonly used distributions for modeling of process fluctuations (uniform, Gaussian, log-normal etc.) can be transformed into a  $N(\mathbf{0}, \mathbf{I})$ -distribution, this assumption imposes no restrictions to the algorithm.

We use a linear model for  $\mathbf{o}$  and  $f$

$$\bar{\mathbf{o}}(\mathbf{s}) = \mathbf{S} \cdot \mathbf{s} + \mathbf{o}_0 \quad (3)$$

$$\bar{f}(\mathbf{s}) = \mathbf{g}^T \cdot \mathbf{s} + f_0 \quad (4)$$

Each test point corresponds to a set of rows in  $\mathbf{S}$ . After performing the test measurement, a Maximum-Likelihood (ML) estimator for  $f$  is

$$\hat{f}(\mathbf{o}') = \mathbf{g}^T \cdot \mathbf{S}^+ \cdot (\mathbf{o}' - \mathbf{o}_0) + f_0, \quad (5)$$

where  $\mathbf{S}^+$  is the pseudo-inverse of the measurement sensitivity matrix  $\mathbf{S} = \nabla_{\mathbf{s}} \mathbf{o}$ , i.e.

$$\min_{\mathbf{s}} \|\mathbf{S} \cdot \mathbf{s} + \mathbf{o}_0 - \bar{\mathbf{o}}\|^2 \Rightarrow \mathbf{s} = \mathbf{S}^+ \cdot (\bar{\mathbf{o}} - \mathbf{o}_0) \quad (6)$$

If  $\mathbf{S}$  has full column rank, then  $\mathbf{S}^+ = (\mathbf{S}^T \mathbf{S})^{-1} \mathbf{S}^T$ . The influence of some parameters could be indistinguishable from the influence of others, i.e. some parameters form an ambiguity group [4, 21]. In this case columns of  $\mathbf{S}$  are linearly dependent, i.e.  $\mathbf{S}$  is rank deficient. So,  $\mathbf{S}^+$  has to be calculated by means of a singular value decomposition (SVD):

$$\mathbf{S} = \mathbf{U} \mathbf{W} \mathbf{V}^T \quad (7)$$

$$\mathbf{S}^+ = \mathbf{V} \mathbf{W}^+ \mathbf{U}^T \quad (8)$$

$$\mathbf{W} = \text{diag}(\sigma_1, \dots, \sigma_r, 0, \dots, 0) \quad (9)$$

$$\mathbf{W}^+ = \text{diag}(1/\sigma_1, \dots, 1/\sigma_r, 0, \dots, 0) \quad (10)$$

The estimation error due to measurement errors  $\boldsymbol{\varepsilon}$  is then

$$\begin{aligned} \eta(\mathbf{s}, \boldsymbol{\varepsilon}) &= \hat{f}(\bar{\mathbf{o}}(\mathbf{s}) + \boldsymbol{\varepsilon}) - \bar{f}(\mathbf{s}) \\ &= \mathbf{g}^T \cdot ((\mathbf{S}^+ \cdot \mathbf{S} - \mathbf{I}) \cdot \mathbf{s} + \mathbf{S}^+ \cdot \boldsymbol{\varepsilon}) \end{aligned} \quad (11)$$

The mean value  $\mathcal{E}\{\eta^2\} = \sigma_{\eta}^2$  of the squared estimation error is used as a quality measure for test selection:

$$\mathcal{E}\{\eta^2\} = \|\mathbf{h}\|^2 + \|\mathbf{g} - \mathbf{S}^T \cdot \mathbf{h}\|^2 \quad (12)$$

$$\mathbf{h} = \mathbf{S}^{T+} \cdot \mathbf{g} \quad (13)$$

If  $\mathbf{S}$  has full column rank, the second summand of (12) vanishes. Since the case of a rank-deficient sensitivity matrix  $\mathbf{S}$  is included in (12), the influence of ambiguity groups [21] in the set of statistical parameters is systematically contained in the optimization goal without the need for a special treatment. Those statistical parameters that have a large impact on the specified performance  $f$  are estimated more precisely than others that are of minor influence on  $f$ .

The optimization algorithm starts with an empty selection, i.e.  $\mathbf{S} = \mathbf{0}$  and  $\mathcal{E}\{\eta^2\} = \|\mathbf{g}\|^2$ , and greedily includes new test points aiming at decreasing  $\mathcal{E}\{\eta^2\}$  for the first specified performance  $f_1$  most rapidly. If the maximum possible relative improvement drops below a given bound (20% used in the example), the algorithm switches to the next specified performance, starting with the current selection. For the example shown in Section 5, the CPU time needed to perform the test point selection was negligible in comparison to the simulation times.

### 3.2 Calculation of the test criterion

Each set of values for the statistical parameters  $\mathbf{s}$  results in either a good or a faulty circuit. The regions of statistical parameter sets leading to good resp. faulty circuits,  $\Omega_g$  resp.  $\Omega_f$ , are defined by:

$$\Omega_g = \{\mathbf{s} \mid f(\mathbf{s}) \geq f_b\} \quad (14)$$

$$\Omega_f = \{\mathbf{s} \mid f(\mathbf{s}) < f_b\} \quad (15)$$

In this paper, the go/no-go test decision for a single performance  $f$  is based on a linear combination  $d$  of the characteristic observations  $\mathbf{o}$  of the DUT [8].

$$d(\mathbf{o}) = \boldsymbol{\theta}^T \cdot \mathbf{o} + \theta_0 \quad (16)$$

$$\mathbf{o}' = \mathbf{o} + \boldsymbol{\varepsilon} \quad (17)$$

A DUT is assumed to meet the specification  $f \geq f_b$ , if  $d(\mathbf{o}') \geq 0$ , else it is rejected. Without loss of generality,  $\boldsymbol{\varepsilon} \sim N(\mathbf{0}, \mathbf{I})$  and  $\|\boldsymbol{\theta}_i\|^2 = 1$  is assumed. Then, pdf( $d(\mathbf{o}') \mid \mathbf{o}$ ) conforms to a Gaussian distribution with mean  $d(\mathbf{o})$  and variance 1.

For a perfect test, the conditions

$$f(\mathbf{s}) \geq f_b \Leftrightarrow \mathbf{s} \in \Omega_g \stackrel{!}{\Leftrightarrow} d(\mathbf{o}') \geq 0 \quad (18)$$

are fulfilled. Due to noise and measurement errors, (18) cannot be achieved, even if the specified performance was included in the set of measurements. Furthermore, non-linearities of the functions  $f(\mathbf{s})$  and  $\mathbf{o}(\mathbf{s})$  inhibit a perfect separation of good and faulty circuits by measuring  $\mathbf{o}$ . Hence, every possible decision rule based on measurements yields a certain *fault coverage*  $f_c$ , that is the percentage of correctly classified faulty circuits among all faulty circuits, and a certain *yield coverage*  $y_c$ , which is the percentage of correctly classified fault-free circuits among all fault-free ones. For a sample DUT with statistical parameters  $\mathbf{s}$ , the probabilities of acceptance  $p_a$  resp. of rejection  $p_r$  are

$$\begin{aligned} p_a(\mathbf{s}, \boldsymbol{\theta}, \theta_0) &= P\{d(\mathbf{o}', \boldsymbol{\theta}, \theta_0) \geq 0 \mid \mathbf{s}\} \\ &= \frac{1}{\sqrt{2\pi}} \int_{-d(\mathbf{o}(\mathbf{s}), \boldsymbol{\theta}, \theta_0)}^{\infty} \exp(-\tau^2/2) d\tau \end{aligned} \quad (19)$$

$$p_r(\mathbf{s}, \boldsymbol{\theta}, \theta_0) = 1 - p_a(\mathbf{s}, \boldsymbol{\theta}, \theta_0) \quad (20)$$

and the yield coverage and fault coverage are

$$y_c(\boldsymbol{\theta}, \theta_0) = \frac{1}{Y} \int_{\Omega_g} p_a(\mathbf{s}, \boldsymbol{\theta}, \theta_0) \cdot \text{pdf}(\mathbf{s}) \, ds$$

$$= \mathcal{E}\{p_a(\mathbf{s}, \boldsymbol{\theta}, \theta_0) \mid \mathbf{s} \in \Omega_g\} \quad (21)$$

$$f_c(\boldsymbol{\theta}, \theta_0) = \frac{1}{1 - Y} \int_{\Omega_f} p_r(\mathbf{s}, \boldsymbol{\theta}, \theta_0) \cdot \text{pdf}(\mathbf{s}) \, ds$$

$$= \mathcal{E}\{p_r(\mathbf{s}, \boldsymbol{\theta}, \theta_0) \mid \mathbf{s} \in \Omega_f\} \quad (22)$$

given the parametric yield  $Y = P\{\mathbf{s} \in \Omega_g\}$ .

Goal of the test design is to minimize the overall test cost, which is determined by the number and kind of test measurements needed and by the probabilities of misclassification. Important figures are the proportion of good circuits that will fail the test (“yield loss”) [23]

$$Y_L = 1 - y_c, \quad (23)$$

and the proportion of faulty circuits that will pass the test

$$F_L = 1 - f_c, \quad (24)$$

which could be called “*fault loss*” accordingly to yield loss. Note that “faulty” means, that a particular circuit fails to meet the specification  $f \geq f_b$ . However, in order to consider the severity of the failure, the *maximum relative deviation from the spec* of all undetected faulty circuits MRD,

$$\text{MRD} = \max_{\substack{\mathbf{s} \in \Omega_f \\ d(\mathbf{o}(\mathbf{s})) \geq 0}} \left| \frac{f(\mathbf{s}) - f_b}{f_b} \right|, \quad (25)$$

is introduced. The MRD shows how close the performance of the misclassified faulty circuits is to the specification boundary. If the MRD lies within the noise and measurement error range of a conventional functional test, then a test based on characteristic observations may be acceptable, independent from  $F_L$ . The concept of fault and yield coverage is therefore enhanced by MRD.

For a given set of measurements, test optimization is minimizing an arbitrary cost function  $q(F_L, Y_L)$  over  $\boldsymbol{\theta}$  and  $\theta_0$ . In the following, the mean of the error probabilities  $q = (Y_L + F_L)/2$  is used. At each of the selected test points,  $\mathbf{o}$  and  $f$  are simulated for a number of sample circuits. The circuits are classified as good or faulty. The test criterion  $d(\boldsymbol{\theta}, \theta_0)$  is determined by minimizing  $q$  over  $\boldsymbol{\theta}$  and  $\theta_0$ . The minimization algorithm uses first and second order derivatives of  $q$ , that are estimated by Monte-Carlo methods applied to the integrals (21), (22) and

$$dq = -(df_c + dy_c)/2$$

$$= -0.5 \cdot \left( \frac{1}{1 - Y} \int_{\Omega_f} dp_r(\mathbf{s}, \boldsymbol{\theta}, \theta_0) \cdot \text{pdf}(\mathbf{s}) \, ds \right.$$

$$\left. + \frac{1}{Y} \int_{\Omega_g} dp_a(\mathbf{s}, \boldsymbol{\theta}, \theta_0) \cdot \text{pdf}(\mathbf{s}) \, ds \right), \quad (26)$$

and similarly for second derivatives. As a consequence of using the non-deterministic fault model, these estimations are continuous functions of  $\boldsymbol{\theta}$  and  $\theta_0$ .

Commonly, there are more than one specified performance. The overall test criterion is a combination of the partial criteria  $d_i$  of the single performances  $f_i$

$$\forall_i d_i(\boldsymbol{\sigma}') \geq 0 \Rightarrow \text{accept DUT, else reject.} \quad (27)$$

In this section, the calculation of a test criterion for a single performance  $f_i$  has been shown.

#### 4 Generation of samples

If the samples used by the discrimination analysis are drawn from their original distribution  $N(\mathbf{s}_0, \mathbf{C})$ , only few faulty samples will occur, facing many good samples. For the robustness and efficiency regarding the total number of necessary samples, it is desirable to have a large number of samples in each

class [24]. Hence, we propose to enrich the sample set with samples drawn from a second distribution  $N(\mathbf{s}_{wc}, \mathbf{C})$  centered around the *worst-case point*  $\mathbf{s}_{wc}$ , as parametric faults most probably occur at  $\mathbf{s} \approx \mathbf{s}_{wc}$  [25]. Taking  $n_0$  samples from  $N(\mathbf{s}_0, \mathbf{C})$  and  $n_1$  samples from  $N(\mathbf{s}_{wc}, \mathbf{C})$ , the overall probability density function is

$$\text{pdf}^*(\mathbf{s}) = (n_0 \cdot \text{pdf}_0(\mathbf{s}) + n_1 \cdot \text{pdf}_1(\mathbf{s})) / (n_0 + n_1). \quad (28)$$

When estimating figures like  $y_c$  and  $f_c$  with samples generated using  $\text{pdf}^*$ , it has to be taken into account, that the sample generating distribution is different from the original distribution:

$$\hat{y}_c(\boldsymbol{\theta}, \theta_0) = \frac{\sum_{\mathbf{s} \in \Omega_g} p_a(\mathbf{s}, \boldsymbol{\theta}, \theta_0) \cdot w(\mathbf{s})}{\sum_{\mathbf{s} \in \Omega_g} w(\mathbf{s})} \quad (29)$$

$$\hat{f}_c(\boldsymbol{\theta}, \theta_0) = \frac{\sum_{\mathbf{s} \in \Omega_f} p_r(\mathbf{s}, \boldsymbol{\theta}, \theta_0) \cdot w(\mathbf{s})}{\sum_{\mathbf{s} \in \Omega_f} w(\mathbf{s})} \quad (30)$$

$$w(\mathbf{s}) = \text{pdf}_0(\mathbf{s}) / \text{pdf}^*(\mathbf{s}) \quad (31)$$

## 5 Results

The example circuit is a CMOS differential bandpass filter consisting of 41 transistors. Table 1 shows two specifications that are defined for this circuit: center frequency and quality. The signal used as a test stimulus is shown in Figure 2. Two parameters  $T_0$  and  $T_1$  determine its shape. The rise time and fall time are both 200ps. This signal can be created by digital circuitry, so that no external signal generation is necessary, and more important, the DUT doesn’t have to be controllable from outside the system. A certain set of possible stimuli parameter values is determined by the signal generation hardware, here  $1/T_0 \in \{50\text{kHz}, 88.9\text{kHz}, 158\text{kHz}, 281\text{kHz}, 500\text{kHz}\}$  and  $T_1/T_0 \in \{0.100, 0.525, 0.950\}$ , yielding 15 test points to choose from. The test stimuli are applied to the DUT and the circuit’s behavior is simulated for  $4T_0$ . Both output signals  $g_p$  and  $g_n$  are sampled with 1MSamples/s and are quantized with 10-bit resolution between 0 and 5V. The quantization error determines  $\varepsilon$  in (17).

Performance	Spec.	Nom. Value	Partial Yield
$f_0$ [MHz]	> 17.5	19.57	87.0%
$Q$	> 15.5	20.4	96.7%

Table 1: Specifications of the circuit example for temperature  $-15^\circ\text{C} < \text{Temp} < +55^\circ\text{C}$  and supply voltage  $4.8\text{V} < V_{DD} < 5.5\text{V}$ .

The test selection procedure presented in Section 3.1 reduced the number of test points to consider from 15 to 5. Two different sets of 350 samples each were used for calculating the test criteria and for validating them. Performing all necessary simulations took 3.5h on a network of 20 Intel PII 350MHz PC’s using the Infineon in-house simulator TITAN [26] and the circuit synthesis tool WICKED [27].

Tables 2 and 3 show the achieved fault loss  $F_L$  and yield loss  $Y_L$  for each specification and for different transform options: time-domain (—), Fourier, and wavelet. Using wavelet transform for test significantly decreased yield loss and fault loss in comparison to Fourier transform or time-domain measurements. In comparison to Fourier transform, wavelet transform reduces the number of faulty circuits passing the test ( $F_L$ ) for the first specification by nearly 50%, and reduces the yield loss by more than 50%. In comparison to time-domain measurements, wavelet transform leads to a 70% reduction in undetected faulty circuits ( $F_L$ ) and a 80% reduction in yield loss  $Y_L$ .

For the second performance “quality”, the differences in  $F_L$  and  $Y_L$  between training and validation sample is nearly as large as the change achieved by choosing a different transform. The test quality for this performance is however improved by employing wavelet transform.

As can be seen in column “MRD”, the faulty circuits that mistakenly pass the test lie nevertheless close to the specification boundary and are almost fault free. The delivered faulty circuits fail the specification by less than 2% (center frequency) resp. 4% (quality), whereas the rejected faulty circuits exceeded their specification by up to 19%. This shows that although there is some fault loss  $F_L$  for circuits that almost fulfill the spec, this test method detects all circuits that violate it more than slightly.

	$F_L$		$Y_L$		MRD
	training	valid.	training	valid.	
—	6.8%	5.7%	13.9%	14.1%	1.5%
Fourier	4.3%	3.3%	7.2%	6.0%	0.3%
Wavelet	1.6%	0.8%	2.7%	2.5%	0.0%

Table 2: Fault and yield loss for specification “center frequency”

	$F_L$		$Y_L$		MRD
	training	valid.	training	valid.	
—	7.0%	8.8%	7.2%	7.3%	3.2%
Fourier	6.1%	5.5%	7.2%	7.3%	1.1%
Wavelet	4.3%	6.4%	7.4%	7.5%	3.2%

Table 3: Fault and yield loss for specification “quality”

To show the efficiency of the proposed optimization of  $q$ , it has been replaced by a conventional Fisher linear discriminant analysis (lda) for comparison. Table 4 shows that direct minimization of the proposed goal  $q$  with a quadratic optimization approach reduces fault loss and yield loss significantly.

Algorithm	center freq.		quality	
	$F_L$	$Y_L$	$F_L$	$Y_L$
lda	8.6%	9.3%	31.8%	44.2%
$q$	0.8%	2.5%	6.4%	7.5%

Table 4: Discrimination algorithms

## 6 Conclusion

A new approach to test parametric faults in analog components of mixed-signal circuits has been presented. It has been shown, that particular properties of the wavelet transformation are advantageous for mixed-signal test with digital test stimuli. This has been demonstrated on an analog CMOS filter circuit, where the test quality figures for measurements after wavelet transform showed to be significantly better than after Fourier transform or with pure time-domain measurements.

We presented a new efficient method for test measurement selection and quadratic test optimization for a parametric fault model that is based on the specification of the circuit. Our method systematically considers measurement errors and parameter ambiguity groups. The presented test design methodology allows testing for parametric faults by means of test equipment that does not have to surpass the DUT in speed and precision.

### Acknowledgment

This work was supported in part with funds of the Deutsche Forschungsgemeinschaft under reference number AN 125/16-2 within the priority program “Design and design methodology of embedded systems.”

## References

[1] Linda S. Milor, “A tutorial introduction to research on analog and mixed-signal circuit testing,” *IEEE Transactions on Circuits and Systems II: Analog and Digital Signal Processing*, vol. 45, no. 10, pp. 1389–1407, Oct. 1998.

[2] “Mixed-signal BIST,” [http://www.logicvision.com/solution/tb\\_msibist.htm](http://www.logicvision.com/solution/tb_msibist.htm).

[3] L. Milor and A. L. Sangiovanni-Vincentelli, “Minimizing production test time to detect faults in analog circuits,” *IEEE Transactions on Computer-Aided Design of Circuits and Systems*, vol. 13, pp. 796–813, 1994.

[4] G. Hemink, B. Meijer, and H. Kerkhoff, “Testability analysis of analog systems,” *IEEE Transactions on Computer-Aided Design of Circuits and Systems*, vol. 9, pp. 573–583, 1990.

[5] Zhihua Wang, Georges Gielen, and Willy Sansen, “Probabilistic fault detection and the selection of measurements for analog integrated circuits,” *IEEE Transactions on Computer-Aided Design of Circuits and Systems*, vol. 17, no. 9, pp. 862–872, 1998.

[6] Giri Devarayanadurg, Mani Soma, Prashant Goteti, and Sam D. Huynh, “Test set selection for structural faults in analog IC’s,” *IEEE Transactions on Computer-Aided Design of Circuits and Systems*, vol. 18, no. 7, pp. 1026–1038, July 1999.

[7] Sam D. Huynh, Seongwon Kim, Mani Soma, and Jinyan Zhang, “Automatic analog test signal generation using multifrequency analysis,” *IEEE Transactions on Circuits and Systems II: Analog and Digital Signal Processing*, vol. 46, no. 5, pp. 565–576, May 1999.

[8] Walter M. Lindermeir, Helmut E. Graeb, and Kurt J. Antreich, “Analog testing by characteristic observation inference,” *IEEE Transactions on Computer-Aided Design of Circuits and Systems*, vol. 18, no. 9, pp. 1353–1368, Sept. 1999.

[9] Chen-Yang Pan and Kwang-Ting (Tim) Cheng, “Test generation for linear time-invariant analog circuits,” *IEEE Transactions on Circuits and Systems II: Analog and Digital Signal Processing*, vol. 46, no. 5, pp. 554–564, May 1999.

[10] M. Ohletz, “Hybrid built-in self-test for mixed analog/digital integrated circuits,” in *European Test Conference (ETC)*, 1991, pp. 307–316.

[11] Evan M. Hawrysh and Gordon W. Roberts, “An integration of memory-based analog signal generation into current DFT architectures,” in *IEEE International Test Conference (ITC)*, 1996, pp. 528–537.

[12] Jeongjin Roh and Jacob A. Abraham, “Subband filtering scheme for analog and mixed-signal circuit testing,” in *IEEE International Test Conference (ITC)*, 1999, pp. 221–229.

[13] P. N. Variyam, A. Chatterjee, and N. Nagi, “Low-cost and efficient digital-compatible BIST for analog circuits using pulse response sampling,” in *15th IEEE VLSI Test Symposium*, 1997, pp. 261–266.

[14] K. Arabi and B. Kaminska, “Oscillation built-in self test (OBIST) scheme for functional and structural testing of analog and mixed-signal integrated circuits,” in *IEEE International Test Conference (ITC)*, 1997, pp. 786–795.

[15] Ingrid Daubechies, “Orthonormal bases of compactly supported wavelets,” *Comm. Pure Appl. Math.*, vol. 41, no. 7, pp. 909–996, 1988.

[16] Sven Simon, Peter Rieder, and Josef A. Nossek, “Efficient VLSI suited architectures for discrete wavelet transforms,” in *VLSI Signal Processing*, vol. IX, pp. 388–397. IEEE, New York, NY, USA, 1996.

[17] B. R. Epstein, M. Czigler, and S. R. Miller, “Fault detection and classification in linear integrated circuits: An application of discrimination analysis and hypothesis testing,” *IEEE Transactions on Computer-Aided Design of Circuits and Systems*, vol. 12, pp. 102–113, 1993.

[18] Chieh-Yuan Chao, Hung-Jen Lin, and Linda Milor, “Optimal testing of VLSI analog circuits,” *IEEE Transactions on Computer-Aided Design of Circuits and Systems*, vol. 16, no. 1, pp. 58–77, Jan. 1997.

[19] F. Bouwman, T. Zwemstra, S. Hartanto, and K. Baker, “Application of joint time-frequency analysis in mixed signal testing,” in *IEEE International Test Conference (ITC)*, 1994, pp. 747–756.

[20] Takahiro Yamaguchi, “Static testing of ADCs using wavelet transform,” in *Sixth Asian Test Symposium*, 1997, pp. 188–193.

[21] G. N. Stenbakken, T. M. Souders, and G. W. Stewart, “Ambiguity groups and testability,” *IEEE Transactions on Instrumentation and Measurement*, vol. 38, no. 5, pp. 941–947, Oct. 1989.

[22] J. V. Spaandonk and T. A. M. Kevenaar, “Selecting measurements to test the functional behavior of analog circuits,” *Journal of Electronic Testing*, vol. 9, pp. 9–18, 1996.

[23] Stephen Sunter and Naveena Nagi, “Test metrics for analog parametric faults,” in *17th IEEE VLSI Test Symposium*, 1999, pp. 226–234.

[24] J. A. Anderson, “Separate sample logistic discrimination,” *Biometrika*, pp. 19–35, 1972.

[25] K. Antreich, H. Graeb, and C. Wieser, “Circuit analysis and optimization driven by worst-case distances,” *IEEE Transactions on Computer-Aided Design of Circuits and Systems*, vol. 13, no. 1, pp. 57–71, Jan. 1994.

[26] U. Feldmann, U. Wever, Q. Zheng, R. Schultz, and H. Wriedt, “Algorithms for modern circuit simulation,” *Archiv für Elektronik und Übertragungstechnik (AEÜ)*, vol. 46, pp. 274–285, 1992.

[27] K. Antreich, J. Eckmueller, H. Graeb, M. Pronath, F. Schenkel, R. Schwencker, and S. Zizala, “WiCkeD: Analog circuit synthesis incorporating mismatch,” in *IEEE Custom Integrated Circuits Conference (CICC)*, 2000.